AUTHOR(S)
Sheludiakov, S., Wetzel, C. K., Lee, D. M., Khmelenko, V. V., Järvinen, J., Ahokas, J., & Vasiliev, S.

TITLE
Spatial Diffusion of Hydrogen Atoms in Normal and Para-Hydrogen Molecular Films at Temperature 0.7 K

YEAR
2024

DOI
10.1007/s10909-024-03053-w

CITATION
Sheludiakov, S., Wetzel, C. K., Lee, D. M., Khmelenko, V. V., Järvinen, J., Ahokas, J., & Vasiliev, S. (2024). *Spatial Diffusion of Hydrogen Atoms in Normal and Para-Hydrogen Molecular Films at Temperature 0.7 K*. Journal of Low Temperature Physics, 215(5–6), 336–356. https://doi.org/10.1007/s10909-024-03053-w

VERSION
Accepted Manuscript

Spatial diffusion of hydrogen atoms in normal and para-hydrogen molecular films at temperature 0.7 K

S. Sheludiakov[1*], C. K. Wetzel[2], D. M. Lee[2], V. V. Khmelenko[2], J. Järvinen[3,4], J. Ahokas[3], S. Vasiliev[3]

[1*]Department of Physics and Astronomy, University of Notre Dame, Notre Dame, 46556, IN, USA.

[2]Institute for Quantum Science and Engineering, Department of Physics and Astronomy, Texas A&M University, College Station, 77843, TX, USA.

[3]Department of Physics and Astronomy University of Turku, Turku, 20014, Finland.

[4] Present address: Bluefors Oy, Arinatie 10, Helsinki, 00370, Finland.

*Corresponding author(s). E-mail(s): ssheludi@nd.edu;

Abstract

We report on electron spin resonance studies of H atoms stabilized in solid H_2 films at temperature 0.7 K and in a magnetic field of 4.6 T. The H atoms were produced by bombarding H_2 films with 100 eV electrons from a radiofrequency discharge run in the sample cell. We observed a one order of magnitude faster H atom accumulation in the films made of para-H_2 gas with a small ortho-H_2 concentration (0.2% ortho-H_2) as compared with those made from normal H_2 gas content (75% ortho-H_2). We also studied the influence of ortho-H_2 molecules on spatial diffusion of H atoms in solid H_2 films. The spatial diffusion of H atoms in both normal and para H_2 films is faster than the diffusion obtained from the measurement of H atom recombination. The rate of spatial diffusion of H atoms in para-H_2 films was slower in comparison with that in the normal H_2 films. We discuss possible explanations of these observations.

Keywords: Solid molecular hydrogen, Hydrogen atoms, diffusion, Electron spin resonance

Introduction

Hydrogen atoms embedded in solid molecular hydrogen represent a special type of quantum solid. Pure solid molecular hydrogen is characterized by the de Boer parameter equal to 1.23 [1] and demonstrates unique quantum properties. There are two possible values for the total nuclear spin, I, of a hydrogen molecule: I=0 and I=1 [2]. Molecules with a nuclear spin I=0 are para-molecules and molecules with a nuclear spin I=1 are ortho-molecules. The wavefunctions of para-molecules have a spherical symmetry, whereas the wavefunctions of ortho-molecules have a p-shape and can be considered as defects in a solid para-H_2 lattice. Normal molecular hydrogen corresponds to an ortho-para composition of H_2 gas at 300 K and contains 25% of para-H_2 and 75% of ortho-H_2. The lowest energy state of para-H_2 is 170.5 K lower than that for ortho-H_2 [2]. After normal solid molecular hydrogen is cooled down to low temperatures, the process of ortho-para conversion takes place with a rate ∼1.9% per hour. Natural ortho-para conversion leads to a reduction of number of ortho-H_2 molecules from 75% to 5% in 40 hours [2, 3]. Initial ortho content in solid H_2 films can be changed by preparing samples from hydrogen gas stored as a liquid in a low-temperature o/p converter packed with a paramagnetic $Fe(OH)_3$ catalyst. The processes of quantum diffusion of ortho-molecules in para-hydrogen were studied by nuclear magnetic resonance (NMR) [4–6] and infrared (IR) spectroscopy methods [7, 8]. The diffusion of ortho-H_2 molecules results in formation of clusters of ortho-molecules (dimers, trimers, and so on) in para H_2 samples [4–6].

Embedding light H atoms in solid H_2 allows creating a system with even more pronounced quantum properties than pure solid hydrogen. The de Boer parameter for a system with H atoms in para H_2 is equal to 2.22 which is even larger than that for solid ^{3}He (2.05) [1]. A hydrogen atom has an electron spin S=1/2 and a nuclear spin I=1/2, which makes it particularly convenient to use methods of NMR and electron spin resonance (ESR) to study processes involving hydrogen atoms. The first studies of H atoms embedded in solid H_2 were performed in the mid- 1950s [9, 10]. The motivation of these studies was an achievement of a high concentration of stabilized H atoms in solid H_2 for the possible application as a rocket fuel. The concentrations of H atoms in solid H_2 of order 7.5% were necessary to achieve an advantage over existing chemical fuels [11]. In these first experiments, the H atom concentrations of order 0.01% were reached thus making impossible practical applications of H-H_2 solid mixtures. It was also found that the small concentrations obtained decreased due to recombination of H atoms in solid H_2 at low temperatures [10].

An interest in studying H atoms in H_2 solids was renewed following a theoretical consideration of quantum diffusion of light impurities in quantum solids [12–14]. It was predicted that at low enough temperatures an impurity inside a crystal becomes delocalized and may freely move within certain energy bands similar to conduction electrons in metals. The phonon-assisted mechanism for so-called physical diffusion of H atoms when they tunnel through the potential barriers in the H_2 crystal lattice was suggested [15]. For the case when a single phonon is involved, a linear dependence for the recombination rate of H atoms in solid H_2 on temperature was first predicted [16] and later observed experimentally in the temperature range 1.3-4.2 K [17–19]. However, measurements of the recombination rate of H atoms in solid H_2 at temperatures

below 1K did not follow a linear temperature dependence and showed a substantial decrease of recombination rate upon lowering temperature below 1 K [20–23].

Alternatively, the migration of H atoms in solid H_2 was explained by the quantum tunneling exchange chemical reaction H+H_2 → H_2 +H [24–26]. This reaction provides a chemical diffusion mechanism for H atoms to move from one lattice site of solid H_2 to another. When introduced into solid hydrogen, H atoms are confined in potential wells in the molecular H_2 lattice. The barrier height for this reaction is 4600 K [27], which is significantly larger than that for the physical diffusion of H atoms in solid H_2 (100 K). On the other hand, the potential barrier for the exchange tunneling reaction H+H_2 →H_2+H is significantly narrower. Theoretical calculations of the rate constant for exchange tunneling reactions of hydrogen atoms in H_2 provide values close to those observed in the experiments [28–30]. Moreover, measurements of the recombination rate of H atoms at temperature 1.3 K and pressures from 0 to 13 MPa did not show any dependence of the recombination rate on pressure [31]. These results could not be explained in the framework of physical diffusion of H atoms which should be suppressed with increasing pressure, thus supporting the mechanism of chemical exchange tunneling of H atoms.

Recombination of H atoms in the H_2 lattice consists of two stages. The first stage is quantum diffusion of H atoms toward each other and the second stage is the recombination when two atoms occupy neighboring positions in the H_2 lattice. There is no barrier for the H atom recombination at the second stage, but to approach each other and reside in the closest lattice sites during the first stage, two H atoms should tunnel through a high barrier. When the H atoms are far from each other, the energy levels of the adjacent lattice sites are equal and the resonant tunneling occurs. However, when two atoms approach each other, the energy levels became distorted by their interactions. The energy level mismatch increases when atoms approach each other and reaches values of order tens of Kelvins for two atoms in the neighboring lattice sites thus slowing down the H atom diffusion towards each other [32]. Previously, all conclusions about the rates of H atom quantum diffusion in solid H_2 were obtained from the measurement of their recombination rates. For the diffusion limited H atom recombination, the relation between recombination rate (k_r) and diffusion coefficient (D_r) is represented by the formula $k_r = 4\pi a_0 D_r$, where a_0 =3.78 Å is a lattice constant of solid H_2. We analyzed all data obtained during measurements of recombination rates for a temperature range 3.6 - 0.15 K and calculated the diffusion coefficients. In this temperature range, the diffusion coefficients obtained from the H atom recombination spanned from 1.6×10^{-17} cm^2s^{-1} to 1.6×10^{-19} cm^2s^{-1} with a tendency to decrease with lowering temperature [17, 19–26, 33–36]. The relative concentrations of H atoms in solid H_2 (n_H/n_{H_2}) were in the range 10^{-4} -10^{-3}. At the same time, it is known that at temperature 0.8 K, the spatial diffusion coefficient, D_{He}, of ^{3}He atoms in solid ^{4}He measured by the NMR spin-echo technique was found to be in the range from 5×10^{-7} cm^2s^{-1} to 5×10^{-10} cm^2s^{-1} when the relative concentration of ^{3}He ($n_{^3He}/n_{^4He}$) was increased from 5×10^{-4} to 5×10^{-2} [37, 38]. The ^{3}He atoms diffused in solid ^{4}He by interchanging their positions with adjacent ^{4}He atoms. This is completely different from the diffusion of H atoms in solid $H_2$where it is governed by the

tunneling exchange chemical reaction. In any case, the observed difference in the values of diffusion coefficients for ^{3}He in solid ^{4}He and for H atoms in solid H_2 obtained from recombination measurements is ten orders of magnitude. We might expect than the pure spatial diffusion of H atoms in solid H_2 is much faster than that obtained from recombination measurements. H atoms can move through the H_2 matrix faster if they avoid one another and do not create mismatches between the energy levels in the neighboring potential wells of the H_2 lattice crystalline field. For the measurements of spatial diffusion, a gradient of H atom concentration should be created, and the process of H-atom propagation into the region with a low H atom concentration should be monitored.

In the first attempt to study spatial diffusion, H atoms were produced in the discharge which was applied in the vicinity of a solid H_2 sample placed in the X-band ESR cavity [39]. Initially, the H atoms were produced in a less sensitive part of the ESR cavity. After waiting for 100 hours, the H atoms diffused towards the most sensitive central part of the cavity, and the H-atom ESR signal was observed. The H atom concentration obtained from the ESR spectra was of order $n_H \sim 10^{15}$ cm^{-3}. These studies indicated a process of the H-atom spatial diffusion, but did not provide fully reliable quantitative values for the spatial diffusion rate. Other attempts to measure the pure spatial diffusion of H atoms in solid H_2 at temperature 1.3-4.4 K were based on studying the influence of H atoms on ortho-para conversion [40, 41]. Unfortunately, it was found that small concentrations of H atoms in solid H_2 did not influence natural ortho-para conversion. Recent studies of diffusion-limited chemical reactions of H atoms with simple organic and inorganic molecules trapped in solid para-hydrogen [1, 42–44] presented important evidence for tunneling of H atoms in solid H_2 and the influence of lattice defects on H atom localization, but did not provide any information on pure spatial H atom diffusion.

In our recent work, we performed the first measurements of the pure H atom spatial diffusion in solid H_2 at temperature 0.7 K [45–47]. We measured two different diffusion coefficients of H atoms in solid H_2 in the same experiment. From studying recombination of H atoms, the recombination diffusion coefficient D_r was calculated. Additionally, we determined the spatial diffusion coefficient, D_{sp}, by studying propagation of H atoms created at the film surface deeper into the film bulk. The coefficient of spatial diffusion of H atoms in normal solid H_2 was found to be more than two-orders-of-magnitude larger than that obtained from the H-atom recombination [45, 46]. These result showed that in the gradient of concentration, H atoms move through the H_2 matrix faster because they avoid one another and do not create an energy level mismatch in the neighboring potential wells of the H_2 lattice crystalline field. In this manuscript, we provide a review of experimental work on studying spatial diffusion of H atoms in solid H_2 and focus on the influence of ortho-H_2 molecules on the H atom accumulation and spatial diffusion in solid H_2.

1 Experimental Setup

A block diagram of the cryogenic part of our experimental setup for studies of quantum diffusion of H atoms in solid H_2 is shown in Fig. 1. The experimental setup is based

on a commercial Oxford 200 dilution refrigerator. The sample cell (SC) is attached to the refrigerator mixing chamber and located in the center of a 4.6 T superconducting magnet and can be cooled down to 100 mK [48, 49]. In order to perform experiments in a magnetic field gradient, we arranged a separate gradient coil assembly able to create in the SC an axial magnetic field gradient of up to ˜ 30 G/cm. The SC consists of the main volume with an open design 128 GHz ESR Fabry-Pérot (FP) resonator and a 910 MHz NMR helical resonator (HNMR) (see Fig. 2a and 2b) [49]. The top spherical ESR resonator mirror is made of silver-plated polycrystalline copper, while the flat bottom mirror is a gold film with a thickness of 400 nm deposited on a single-crystal quartz disc. The flat mirror also acted as the top electrode of a quartz microbalance (QM) [49]. Such a SC design made it possible for us to simultaneously measure the H_2 film thickness by the QM and detect H atoms by means of the 128 GHz ESR spectrometer [50].

The sample cell design also allows a two-stage ESR resonator frequency tuning. First, we performed a coarse (up to 10 GHz) frequency adjustment at room temperature using a miniature bronze bellows (Fig. 2a) and a set of fixing screws [49]. In addition to that, the cavity frequency could be fine-tuned *in situ* at low temperatures ($\Delta f \simeq 1$ GHz) using a system of edge-welded stainless-steel bellows and a titanium Attocube ANPz101/LT piezo positioner.

The FP ESR resonator is connected to a 128 GHz ESR spectrometer [50] through a waveguide assembly. The H NMR coil was used to create H atoms in the H_2 films by running a discharge in helium gas in SC as well as to initiate an NMR transition of H atoms in the H_2 films. For running the discharge, a few-watt rf pulses were sent to the H NMR coil with a typical pulse duration of 0.1 ms and duty cycle of 1/200. The electrons created in the discharge have energies of order 100 eV which is enough to dissociate H_2 molecules in a solid hydrogen film in the layer of ∼100 nm [48].

The samples of H atoms in solid H_2 were prepared as follows. First, we condensed a few μmoles of He in the auxiliary volume under the QM. At temperatures of our experiments, helium formed a superfluid film which flushed the bottom QM surface and removed heat released during the sample deposition and recombination of H atoms in the H_2 films. After that, we proceeded to deposit a solid molecular hydrogen film onto the QM top electrode either directly from a room temperature gas-handling system or by re-condensing it from the dissociator chamber (Fig. 2a). In the latter case, we filled the dissociator chamber with a few tens of mmoles of H_2 gas in advance. Then we initiated the film deposition by heating the dissociator to a temperature of 5-6 K. At these temperatures, the H_2 vapor pressure becomes high enough to build up a solid H_2 film on the QM surface. The SC temperature during the film deposition was stabilized at 0.5-1 K with a typical hydrogen gas flow rate, equivalent to the H_2 film growth of about 0.1-1 monolayer/s. Creating thick films of the order of 1 mm required order of magnitude faster rates, which were obtained using the deposition from room temperature gas handling system. Using these regimes, we were aiming to create uniform polycrystalline films with a low local inhomogeneity and thicknesses from a few nanometers to about a millimeter [23].

Unfortunately, the QM performance degraded during the H_2 film deposition. Using the QM, we could measure film thicknesses up to 20 μm. In order to deposit H_2 films of

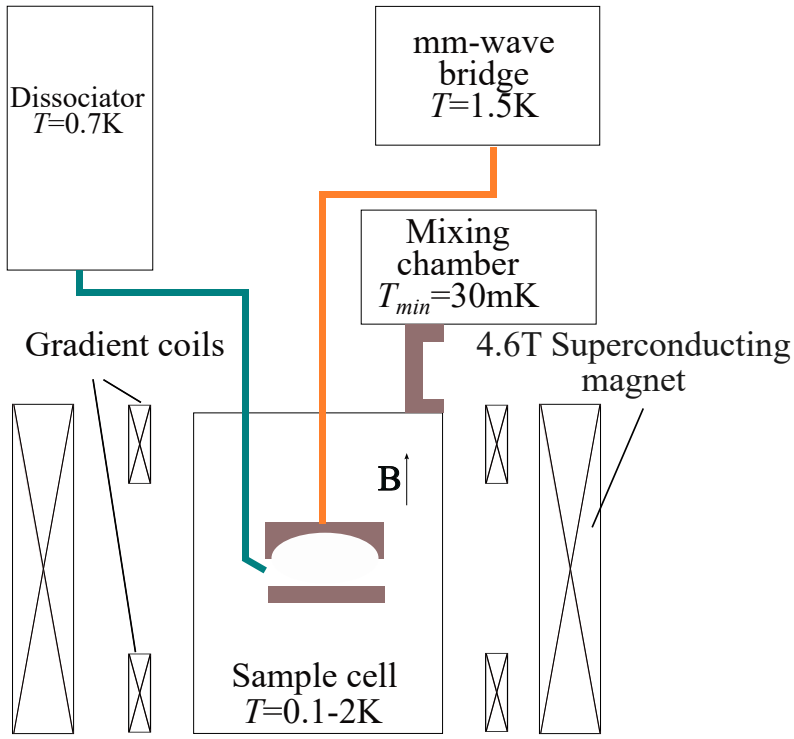

Fig. 1 Block diagram of the experimental setup [23].

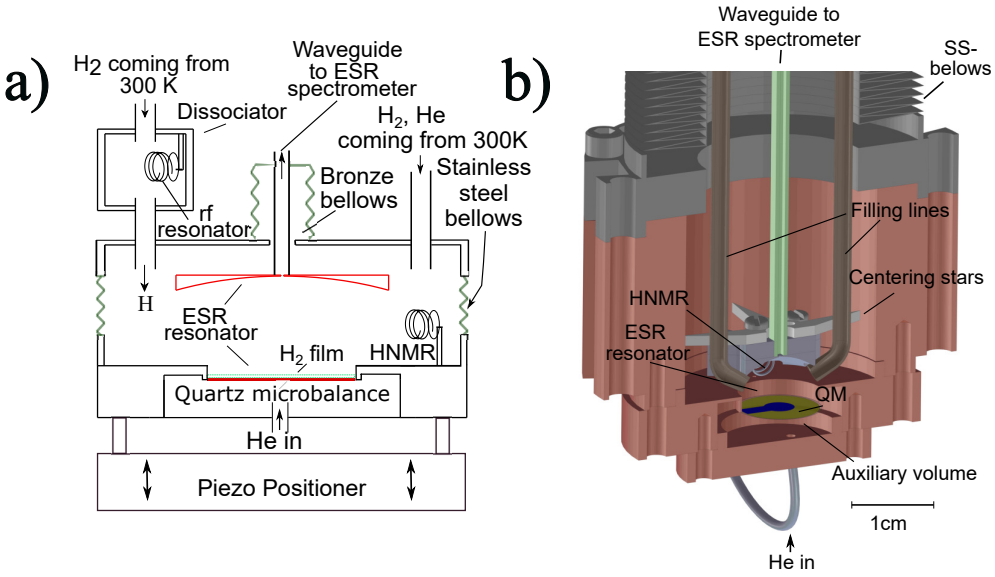

Fig. 2 a) Sample cell schematic, b) Drawing of a lower part of the sample cell [49].

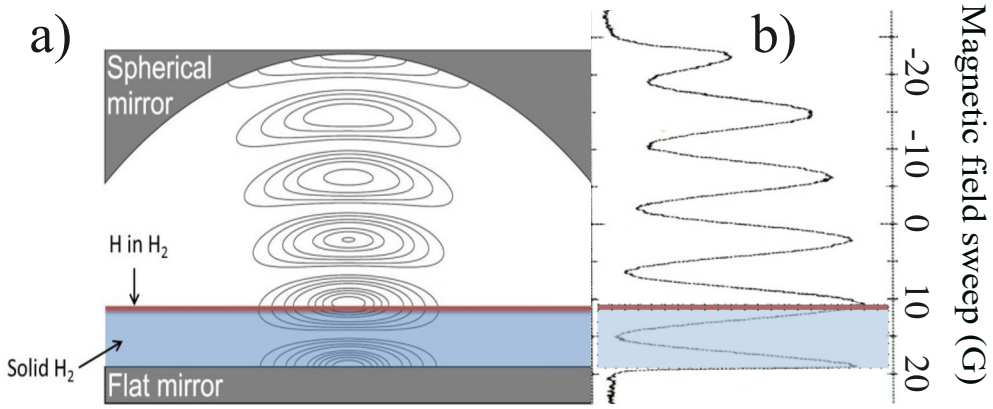

Fig. 3 a) Distribution of mm-wave magnetic field in the Fabry-Perot resonator [23]. Red line corresponds to the ∼100 nm thick layer with H atoms formed just after applying discharge. Blue region corresponds to the thick (∼1.3 mm) layer of solid H_2. b) ESR a-d transition spectra of H atoms in gas phase in axial magnetic field gradient of 25 G/cm. The spectrum reflects the axial profile of the mm-wave H_1 field in the resonator.

a greater thickness, we stabilized the H_2 gas flow in the beginning of deposition using the QM and then continued the accumulation. In this case, the film thickness was estimated from the deposition time considering that the H_2 gas flow into the SC did not change. After creating the H_2 film, we stabilized the SC temperature at T=0.7 K and condensed a few μmoles of helium gas into the SC to start the rf discharge in helium vapor using the helical resonator (HNMR in Fig. 2a and Fig. 2b). The electrons created during the SC discharge bombarded the H_2 films and dissociated a fraction of hydrogen molecules near the surface, thus giving rise to the ESR signals of H atoms in solid H_2.

Our FP resonator operated in the TEM_{005} mode. A profile of the simulated mm-wave field inside the FP resonator is shown in Fig. 3a. The mm-wave field distribution in the FP resonator could also be visualized directly by accumulating atomic hydrogen gas inside the sample cell. The gas-phase H atoms fill the whole SC volume, and their ESR signals measured in the magnetic field gradient directly follow the distribution of the oscillating magnetic field in the cavity (Fig. 3b). As a result, the ESR spectra of gas-phase H atoms have six components when a magnetic field gradient is applied [23]. Each maximum corresponds to an antinode of mm-waves in the resonator. The distance between the spherical and flat mirrors in the resonator is equal to 6.7 mm. The distance between the antinodes is ∼1.3 mm.

Our sample cell and ESR resonator were designed for studies of a spatial diffusion of H in thick H_2 films covering two adjacent maxima of the mm-wave magnetic field above the flat mirror. A typical film thickness should correspond to the antinode separation and, thus, be ∼1.3 mm. The upper surface of an H_2 film should be at the second maximum of the mm-wave field above the flat mirror. By running the discharge in helium gas above the film surface, a layer with a high concentration of H atoms should be created (shown as a red line in Fig. 3a and Fig. 3b). The initial thickness of this layer of H atoms will be equal to ≃100 nm, which is determined by the penetration

depth of electrons from the discharge. By applying a magnetic field gradient, we could study evolution of the ESR signal from H atoms in two adjacent mm-wave maxima: the one at the upper H_2 film surface, and that near the flat mirror, respectively. A registration of the H atom ESR signal from the bottom antinode would provide us with direct evidence for H-atom spatial quantum diffusion. Moreover, time evolution of the ESR line components corresponding to both antinodes would give us quantitative information on the spatial diffusion rate, D_{sp}. Along with the HNMR in the SC, we also arranged a small rf resonator (f=750 MHz) in the hydrogen dissociator chamber (Fig. 2a). By running the rf discharge in the dissociator, we could send a flux of atomic hydrogen gas into the SC volume. We used the ESR signals from H atoms in the gas phase to calibrate the ESR line areas of H atoms in solid H_2 and calculate an absolute number of H atoms in hydrogen films [49]. In this work, we also used a concentration-dependent ESR line broadening due to a dipolar interaction between the electrons spins of H atoms to estimate the local concentrations of hydrogen atoms in the H_2 films [22].

2 Experimental results

In our first attempts to study spatial diffusion of H atoms in solid H_2, we tried to build millimeter thick H_2 films. A $\sim$ 1.3 mm molecular hydrogen film grown on a flat mirror shifts the FP resonator frequency by about 2.5 GHz. Our high frequency ESR spectrometer has a limited frequency range (128$\pm$0.5 GHz) defined by the mm-wave band-pass filter [50]. That is why we developed a SC with the possibility to compensate for a frequency shift resulting from the creation of a thick film.

The ESR frequency adjustment was done in two steps. First, we performed a coarse FP resonator frequency tuning at room temperature before closing the vacuum can of the dilution refrigerator using the bronze bellows and a system of fixing screws. The distance between the mirrors was adjusted in a way such that the SC cooldown and H_2 film deposition would bring the cavity frequency back into the frequency range of our ESR spectrometer. The resonator frequency fine-tuning was performed at low temperature by adjusting the mirror spacing with the piezo positioner. Unfortunately, such a procedure does not allow following the cavity resonance shift all the way upon cool-down and during the film growth, while it is outside the spectrometer bandwidth. After finishing the deposition, the cavity resonance became poor, probably due to the large amount of solid H_2 on the FPR mirrors and cavity coupling orifice. Clear identification of the cavity mode was not possible.

We tried to run the discharge and recorded ESR spectra selecting the best candidate for the cavity mode. We were able to make a registration of H atoms in the gas phase. The ESR lines of the gas phase atoms were very broad and contained several peaks even without applying any magnetic field gradient. This could be a result of a wrong FPR mode identification. No ESR lines were detected after stopping the discharge and destroying gas phase H by recombination. Our attempts to detect H atoms in the solid thick H_2 films were unsuccessful. Similar problems with building a uniform thick H_2 film on the flat mirror of FPR are described in our previous work [51], where we succeeded to create only an order of magnitude thinner ($\sim$ 100μm)

samples of H in H_2. In the course of experiments, it was found that the films of order 0.1-2.5 μm do not create large shifts and disturbances to the FP resonances. H atoms in thin solid H_2 were easily observed, and the process of their accumulation could be studied in great detail. Therefore, we focused our work on studies of samples of the μm size as described below.

Usually, the experiments were performed in the following order. First, we prepared the H_2 film with a thickness of up to 2.5 μm. After that, we added 1 μmol of helium gas into the SC, started the rf discharge and stabilized the SC temperature at $T \sim 0.7$ K. Following that we monitored the ESR signal of H atoms in solid H_2 during a period of time of more than two weeks. We studied eight H_2 films with different thicknesses and different contents of ortho-H_2 molecules from 0.2 to 75% [45, 46]. In this article, we present a comparison of a normal-H_2 (75% ortho-H_2) and para-H_2 film (0.2% ortho-H_2) with a thickness of 2.5 μm to emphasize the influence of ortho-molecules on the H atom accumulation and spatial diffusion. The ESR spectra of H atoms in solid H_2 films grown from normal hydrogen and para-hydrogen are shown in Fig. 4. The ESR spectra of H atoms for these films consist of two asymmetric lines, H_a and H_b, separated by 507 G. Both lines could be represented by a sum of two components, a narrow component (C1 in Fig 4) and a broad component (C2 in Fig. 4). Both doublets of the lines (C1-C1 and C2-C2) are characterized by the same spectroscopic parameters, the electronic g-factor and hyperfine constant A, which correspond to H atoms located in the substitutional sites of the H_2 lattice [45]. The doublets have different linewidths and appear shifted relative to each other. This allowed us to assign these doublets to two ensembles of H atoms with different local concentrations: an ensemble with a low local concentration of H atoms corresponding to the C1-C1 doublet and an ensemble with a high local concentration of H atoms which corresponds to the C2-C2 doublet [45, 51]. Figure 4 shows ESR spectra for H atoms in solid H_2 films after two days of accumulation (a1 and b1) and after seven days of accumulation (a2 and b2). One can see that the broad components of the ESR spectra continued to grow in contrast to the narrow components which stopped changing after two days of accumulation. By monitoring time evolution of the ESR spectra, we followed the local H-atom concentrations and total number of H atoms in the H_2 films by measuring the spectra linewidths and areas, respectively [23, 45]. Time evolution of the broad and narrow components shows that the width of the narrow component (C1) corresponds to the local concentration of 5×10^{18}cm^{-3} (195 ppm) and the width of broad component (C2) corresponds to the local concentration of 1.25×10^{19}cm^{-3} (580 ppm). Since the addition of the narrow component to the linewidth and area of the experimental ESR lines is small and did not change after the first two days of accumulation, we fitted the experimental spectra with a single Lorentzian line. This provided information on the behavior of the region in H_2 films with a high concentration of H atoms.

We studied the H-atom accumulation in both normal and para H_2 films. Figure 5 shows a dependence of the local concentration of H atoms in normal and para-H_2 films on time during the first two days of H atom accumulation. In both films the local concentrations were saturated at the level n_{loc}=1.25×10^{19}cm^{-3}. However, the time to achieve the maximum local concentration was substantially different. In the para-H_2 film, the saturated value was obtained rather fast, after $\sim$5 hours but in

the normal H_2 film this value was achieved after a longer period of ∼2 days. The saturation of local concentration is determined by an equilibrium between the rate of H atom production due to a discharge and their disappearance due to recombination. The rates of atom production were determined at the early stage of accumulation from the slope of the lines shown in Fig. 5 for the condition when recombination of the H atoms was negligible. In the para-H_2 film H atom production rate, k_{pr}, is equal to 10^{15}cm^{3}s^{-1} and in the normal H_2 film H atom production rate is more than one order magnitude lower, k_{pr}=6×10^{13} cm^{3}s^{-1} [46].

A time dependence of the local concentration and absolute number of H atoms in the normal H_2 film during a longer period (16 days) is shown in Fig. 6. From the graphs in Fig. 6 we can find two distinct stages in the H atom accumulation. During the first stage, which lasted 2.5 days, running the discharge led to a linear increase of the H atom local concentration (see Fig. 6a) and absolute number of H atoms in the film. During the second stage which lasted all the remaining 13.5 days of accumulation, the local concentration became saturated and did not increase anymore (see Fig. 6a) although the absolute number of H atoms in the film continued to grow steadily as shown in Fig. 6b.

The ESR line shape and the observed time dependencies of the absolute number of atoms and local concentrations of H atoms in solid H_2 film allowed us to suggest the following qualitative model of H atom accumulation. During the first accumulation stage, a layer of high concentration of H atoms was formed under the H_2 film surface. The energy of electrons produced in the discharge above the H_2 film is 100 eV was sufficient to penetrate into the film and dissociate molecules in the layer within a depth of up to 100 nm. The growing linewidth of the C2 component corresponds to an increasing concentration of H atoms in this 100 nm layer (shown red in Fig. 7a). The narrow C1 component corresponded to H atoms which propagated into the bulk H_2 film beyond the surface layer, forming the front of H atom propagation into the H_2 film bulk (shown pink in Fig. 7a). In this region, the local H atom concentration is smaller than that in the layer with a high concentration of H atoms. At the end of the first stage of accumulation the local concentration is saturated due to equilibrium in the production H atoms and their recombination in the H_2 film. During the second stage the linewidth of C1 and C2 components did not change, providing evidence that the local concentrations in the highly concentrated layer and in the front of this layer are constant. However, the integrals of the C1 and C2 components showed that the number of H atoms in these two different regions of the film behaved completely differently. The C1 component integral was constant, whereas the integral of the broader C2 component continued to grow steadily. This last observation led us to a conclusion that the highly concentrated layer propagates into the H_2 film due to the spatial diffusion and the number of H atoms in the front of the highly concentrated layer did not change during the H atom accumulation. A schematic representation of the H atom propagation into the H_2 film bulk is shown in Fig. 7b and Fig. 7c.

Following this model, we obtained quantitative characteristics for the H atom recombination and spatial diffusion in solid H_2. The H atom concentration change in the film, $dn(t)/dt$, can be described by the following differential equation:

$$dn(t)/dt = k_{pr} - 2k_r n^2(x,t) - D_{sp} d^2 n/dx^2, \quad (1)$$

where k_{pr} is a constant H atom production rate due to running the discharge, k_r is a recombination rate of H atoms in solid H_2, D_{sp} is a coefficient of pure spatial diffusion of H atoms into the bulk H_2 film, and x is the thickness of the H atom high-concentration layer, respectively. An instantaneous H atom concentration can be calculated by solving the differential equation (1). An analysis of the temporal behavior of the local concentrations and absolute numbers of H atoms in solid H_2 films allows us to calculate the above-mentioned characteristics.

At the beginning of H atom accumulation, when their concentrations were low, the recombination and diffusion terms in equation (1) are small. As a result, the first linear term, corresponding to the production of H atoms due to dissociation of H_2 molecules by electron impact, dominates. From the slope of curve in Fig. 6b at the beginning of accumulation, the production rate equal to k_{pr} =6×10^{13}cm^{3}s^{-1} was determined.

As time progressed, the production term eventually becomes compensated by the H atom recombination. This leads to saturation of the H atom local concentration as shown in Fig. 6a. At this first stage, the H-atom diffusion was negligible and the evolution of the H atom concentration in time is described by the first two terms in Eq. (1) [52]. The solution of this simplified equation is as follows:

$$n(t) = n_{eq} tanh(-t/\tau). \quad (2)$$

At the end of the first stage when $dn/dt = 0$, the production and recombination terms become equal, leading to the equilibrium concentration:

$$n_{eq} = \sqrt{k_{pr}/2k_r} \quad (3)$$

with a characteristic time:

$$\tau = 1/\sqrt{2k_{pr}k_r}. \quad (4)$$

We calculated the recombination rate of H atoms in H_2 films as $k_r = k_{pr}/2n_{eq}^2$. The calculated value for k_r is equal to 1.8×10^{-25} cm^{3}s^{-1}. The H atom recombination is a diffusion limited process with $k_r = 4\pi D_r a_0$. The diffusion coefficient for H atom recombination was directly estimated as D_r=4×10^{-19}cm^{2}s^{-1}.

During the second accumulation stage, the intensity of the broad component C2 increased during the discharge, but its width remained constant (see Fig. 6a and Fig. 6b). This corresponded to a gradual increase of the absolute number of H atoms in the H_2 film while the local concentration of H atoms ceased to change. We interpreted this as the propagation of the H atom high-concentration layer into the film bulk which is characterized by the third diffusion term in Eq. (1). We obtained the spatial diffusion coefficient D_{sp} as follows. We first calculated the penetration depth of the H atom high-concentration layer into the H_2 film as a function of time, $x(t)$, using the time dependence of the absolute number of H atoms shown in Fig. 6b and the H atom local concentration. The latter was equal to 1.25×10^{19}cm^{-3} and remained constant during the entire second stage of accumulation.

$$N_{abs}(t) = n_{loc} S x(t). \quad (5)$$

Here N_{abs} is an absolute number of H atoms in the H_2 film, n_{loc} is a local concentration of H atoms in the high-concentration layer, S is the flat mirror surface area where the H_2 film was grown and $x(t)$ is a penetration depth of H atom high concentrated layer into the bulk of the remaining H_2 film. The calculated time dependence of the high concentrated layer penetration depth is shown in Fig. 8. For the analysis of H atom diffusion at the second accumulation stage, we assumed a case of one-dimensional diffusion of H atoms into H_2 film bulk with no radial gradient of H concentration in the film during the discharge. In this case, the penetration depth of H atom high-concentration layer was defined by a solution of Fick's second law as

$$x(t) = \sqrt{2D_{sp}t}. \tag{6}$$

We obtained the value $D_{sp} = 1.5{\times}10^{-16}\mathrm{cm}^2\mathrm{s}^{-1}$ by fitting the experimental data presented in Fig. 8 using Eq. (6). The ratio of two rates: the one of spatial diffusion and that of diffusion leading to H atom recombination, D_{sp}/D_r, measured at the same temperature T=0.7 K and with the condition of an ongoing discharge was found to be 375. This provided evidence that the spatial diffusion measured under the condition when H atoms can avoid approaching each other is considerably faster than that obtained from recombination measurements when H atoms have to approach each other in order to recombine.

For understanding the effect of ortho-H_2 molecules on H atom spatial diffusion, we also performed experiments with para-H_2 films. This allowed us to compare the H atom behavior in para and normal H_2 films. The experiment with a para-H_2 film was performed under conditions identical to those used for the normal H_2 film described above. First, we grew a 2.5 μm thick para-H_2 film on the flat mirror. After that we started the rf discharge in the SC while its temperature was stabilized at 0.7 K. The ESR signal from H atoms in the para-H_2 film was monitored during a time period of 16 days. Time evolution of the local concentration and absolute number of H atoms in the para H_2 film is shown in Fig. 9 with blue filled squares. We also present time evolution of the local concentration and absolute number of H atoms in the normal H_2 film for comparison in Fig. 9 by red filled circles. From Fig. 9a we can see that the maximum H atom local concentrations achieved in the process of accumulation are the same for normal and para-H_2 films, but the rate of achieving this maximum concentration is an order magnitude faster in a para-H_2 film as discussed earlier (see also Fig. 5). During the first six days of accumulation, the absolute number of H atoms in the para-H_2 film is larger than that in normal H_2 film. On the sixth day, the absolute numbers in both films become equal, but after that the absolute number in the normal H_2 film became somewhat larger than that in the para H_2 film (see Fig. 9b).

For analyzing the data for H atoms in para-H_2 film we used the same approach as for the case of H atoms in the normal H_2 film. We calculated the recombination rate of H atoms in the para-H_2 film as $k_r = k_{pr}/2n_{eq}^2$ using data presented in Fig. 9a. The calculated value for k_r for H atoms in para H_2 is equal to $3{\times}10^{-24}\mathrm{cm}^{-3}\mathrm{s}^{-1}$. This value is 16 time larger than that for the normal H_2 film.

From the relation between the recombination rate of H atoms and the diffusion coefficient, the diffusion coefficient D_r was found to be $6{\times}10^{-18}\mathrm{cm}^2\mathrm{s}^{-1}$. The diffusion coefficient due to recombination in the para-H_2 film is 16 times larger than that for

Sample	Normal-H_2 film (75% ortho-H_2)	Para-H_2 film (0.2% ortho-H_2)
$k_{pr}(cm^3s^{-1})$	6×10^{13}	1×10^{15}
$k_r(cm^3s^{-1})$	1.8×10^{-25}	3×10^{-24}
$D_r(cm^2s^{-1})$	4×10^{-19}	6×10^{-18}
$D_{sp}(cm^2s^{-1})$	1.5×10^{-16}	5×10^{-17}
$n(cm^{-3})$	1.3×10^{19}	1.3×10^{19}

Table 1 Concentrations of H atoms, n; constant of H atom production due to discharge, k_p; H atom recombination rate, k_r; diffusion coefficient associated with the H atom recombination, D_r; spatial diffusion coefficient of the H atoms, D_{sp}

the normal H_2 film. To obtain the spatial diffusion coefficient D_{sp}, of H atoms in para-H_2 from Equation (5) we calculated the dependence of the penetration depth of the H atom high-concentration layer into the para-H_2 film, $x(t)$, using the time dependence of n_{abs}, absolute number of H atoms in the para-H_2 film, shown in Fig. 9b, the value of H atom local concentration, which was also equal to n_{loc} =$1.25\times10^{19}cm^{-3}$ (see Fig. 9a), and the known surface area of the H_2 film grown on the flat ESR mirror. The calculated time dependence of the penetration depth of the high-concentration layer into the para-H_2 film is shown in Fig. 10 with blue filled squares. In the same figure, we present a similar dependence for the normal H_2 film with filled squares for comparison. From the fit of the penetration depth of the highly concentrated layer into the para-H_2 film, shown as a solid blue line in Fig. 10, by using the Eq. (6), the value D_{sp} = $5\times10^{-17}cm^2s^{-1}$ was obtained. This value is 3 times smaller than that for H atoms in normal H_2. For H atoms in para H_2, the ratio of coefficients for spatial diffusion and for diffusion due to H atom recombination, D_{sp}/D_r, measured at the same temperature T=0.7 K and in the condition of ongoing discharge is equal to 8.4. Results for accumulation of H atoms in para-H_2 still provide evidence that the spatial diffusion measured under the condition when H atoms can avoid approaching each other is faster than that obtained from recombination measurements when H atoms have to approach each other in order to recombine, but this effect is considerably smaller than for H atoms in normal H_2 films.

We summarized the results obtained for H atom recombination and diffusion coefficients for normal-H_2 and para-H_2 films in Table1.

3 Discussion

We studied the H atom pure spatial and recombination diffusion in 2.5 μm thick normal- and para-H_2 films at temperature T= 0.7 K. In both samples in accordance with our previous publications [46, 47], the spatial diffusion of H atoms was faster than that obtained from the recombination rate of H atoms (see Table1).

It is known from previous studies that the presence of ortho-H_2 molecules in solid H_2 affects the recombination rate of H atoms. The dependence of H atom recombination rate constant on the concentration of ortho-H_2 molecules in solid H_2 was studied earlier at T=4.2 K [34, 35, 53]. It was found that when the concentration of ortho-H_2 molecules in solid H_2 increased from 0.1% to 8%, the recombination rate constant also increased from 8.3×10^{-23} cm^3s^{-1} to $5.4\times10^{-22}cm^3s^{-1}$ but a further increase of the concentration of ortho-H_2 molecules to 75% led to a decrease of the rate constant to

1.17×10^{-22}cm^{3}s^{-1}. In our studies performed at 0.7 K, we compare only the H atom recombination rate constants for two H_2 samples with ortho-H_2 concentrations equal to 0.2% and 75%. The values of recombination rates measured at T=0.7 K are much lower (see Table1) as compared to that measured at T=4.2 K. However, the ratio of rate constants for these H_2 samples, k_r(0.2% ortho-H_2)/k_r(75% ortho-H_2) measured at T=0.7 K is equal to 17 and is much larger than that obtained at T=4.2 K.

This important effect can be explained by differences in the tunneling conditions for spatial and recombination diffusion. For the case of spatial diffusion, a gradient of H atom concentration was created and the H atoms moved by a repetition of the tunneling exchange chemical reaction H+H_2=H_2+H to the region with a low H atom concentration without approaching one another. In this case, the energy levels of H atoms in the neighboring H_2 lattice sites remain equal thus favoring resonant tunneling. In the case of recombination diffusion, we register only the events of H atom recombination when two H atoms have to approach each other in order to recombine. As two H atoms move closer, the mismatch between the energy levels of H atoms in the neighboring H_2 lattice sites increases up to 50 K [32]. The tunneling process slowdown results in decreasing diffusion coefficient determined from the recombination rate of H atoms.

Surprisingly, the spatial diffusion rate for H atoms in para-H_2 films is 3 times smaller than that for normal-H_2 films (see Table 1). This is probably a result of a larger recombination diffusion rate of H atoms in these samples. The recombination diffusion of H atoms in para-H_2 film is an order of magnitude faster than that observed for normal-H_2 samples. During the measurement of the penetration depth of the high-concentration layer, the larger recombination rate of H atoms in para H_2 leads to a more efficient H-atom loss in this layer, resulting in slowing of the propagation rate of this layer compared to that in normal H_2 films.

All measurements were performed for the H atom concentration n_{loc}=1.25×10^{19}cm^{-3}. For this concentration, the process of self-localization can also be expected to be similar to that of ^{3}He atoms in solid ^{4}He [37, 38]. Decreasing the concentration of H atoms in solid H_2 films should reduce the effect of recombination of H atoms on the process of spatial diffusion in para H_2 films as well as diminish the process of H atom self-localization. We might expect a higher rate of spatial diffusion at lower concentrations of H atoms similar to that observed for ^{3}He atoms in solid ^{4}He [38]. Unfortunately, we were unable to find steady-state conditions for studying pure spatial diffusion of H atoms in solid H_2 films while running the discharge able to sustain the H atom concentrations $\sim10^{18}$ or below. We will continue to search for such a regime in our future studies.

Another effect observed in this work is a fast accumulation of H atoms in the para-H_2 samples which is about one order of magnitude higher than that for the accumulation rate of H atoms in normal-H_2 samples (See Fig. 5). At the same time, the maximum concentrations of H atoms achieved in both normal-H_2 and para-H_2 samples were very similar, of order 1.25×10^{19}cm^{-3}. We did not observe any change of the production rate k_{pr} in the normal H_2 film due to the process of continuing stimulated and natural ortho-para conversion of H_2 molecules which significantly decreased ortho-H_2 content in the normal H_2 films during the time interval of two days (Fig. 5). An

independence of the production rate on time within the first 2 days observed in this work also excludes the possibility for different cross sections of para-H_2 and ortho-H_2 molecular dissociation as well as different penetration depths of the discharge electrons into the films. Another possibility for a larger production rate of H atoms in solid para-H_2 might be a slower vibrational relaxation of excited H_2 molecules. It was suggested [53] that the presence of o-H_2 molecules with a nonzero quadrupole moment in the vicinity of an excited H_2 molecule may activate vibrational deexcitation associated with infrared emission. This pathway is prohibited in a pure para-H_2 crystal [54] but can be activated by small ortho-H_2 admixtures of order 1%. In this case, an H_2 molecule in para-H_2 environment after collision with an electron is excited to the dissociation threshold and due to a longer vibrational relaxation time may have a higher probability to split into two H atoms instead of relaxing back to the ground vibrational state. The relaxation of vibrationally excited H_2 molecules in solid H_2 was measured up to the v=3 vibrational level at $T \approx$11 K and did not show a difference in H_2 molecule vibrational relaxation times for para- and normal-H_2 samples (both are of order μs) [55]. Therefore, the observed phenomena of different production rates of H atoms in normal-H_2 and para-H_2 cannot be explained by different vibrational relaxation rates of para-H_2 and ortho-H_2 molecules.

Our qualitative explanation of this effect is following. During the stage of accumulation, H atom pairs formed in an ortho-H_2 rich environment can temporarily become trapped there due to a higher energy level mismatch in the neighboring H_2 lattice sites and, thus, have a higher probability of recombining back. On the other hand, H atom pairs formed in the para-H_2 environment can freely move from each other, providing faster growth of H atom concentration. Interestingly, we observed nearly equal steady-state local concentrations of H atoms for both normal and para- H_2 films, indicating that for the second stage of accumulation, the rate of H atom production due to the discharge is equal to the rate of recombination of H atoms for the films with different ortho-para content. Further studies may provide more insight into this phenomenon.

4 Conclusion

We performed investigations of accumulation and pure spatial diffusion of H atoms in solid normal and para-H_2 films. It was found that the rate of accumulation of H atoms in para-H_2 films is one order of magnitude faster than that in normal H_2 films at the beginning of accumulation.

We also found that spatial diffusion proceeds much faster as compared with the diffusion obtained from H atom recombination measurements. In the normal H_2 films the spatial diffusion is more than two orders of magnitude faster than the diffusion obtained from H atom recombination measurements, but in the para-H_2 films the spatial diffusion is only one order of magnitude faster than the diffusion obtained from H atom recombination measurements. For understanding the influence of ortho-para content of solid H_2 films on accumulation and H atom diffusion in more detail, a combination of the NMR method for monitoring ortho-H_2molecules and the ESR method for controlling the H atom behavior is very promising. The approach developed in our studies allow one to perform measurements of spatial diffusion of atoms and

diffusion due to their recombination in different molecular matrices. In the future we plan to study spatial diffusion of D atoms in D_2 films and H atoms in HD films.

Acknowledgments. This work has been supported by National Science Foundation Grant No. DMR 2104756 and the Academy of Finland Grant No. 317141.

References

[1] Mutunga, F.M., Olenyik, K.M., Strom, A.I., Anderson, D.T.: Hydrogen atom quantum diffusion in solid parahydrogen: The H+N_2O→cis-HNNO→trans-HNNO reaction. J Chem. Phys. **154**(1), 014302 (2021)

[2] Silvera, I.F.: The solid molecular hydrogens in the condensed phase: Fundamentals and static properties. Rev. Mod. Phys. **52**, 393–452 (1980)

[3] Pobell, F.: Matter and Methods at Low Temperatures. Springer, Berlin, Heidelberg (2013)

[4] Amstutz, L.I., Thompson, J.R., Meyer, H.: Observation of molecular motion in solid H_2 below 4.2°K. Phys. Rev. Lett. **21**, 1175–1177 (1968)

[5] Washburn, S., Schweizer, R., Meyer, H.: NMR studies on single crystals of H_2. iii. dynamic effects. J. Low Temp. Phys. **40**, 187–205 (1980)

[6] Meyer, H.: Quantum diffusion and tunneling in the solid hydrogens (a short review). Low Temperature Physics **24**(6), 381–392 (1998)

[7] Boggs, S.A., Welsh, H.L.: An infrared spectroscopic study of quantum diffusion in solid hydrogen. Can. J. Phys. **51**(18), 1910–1914 (1973)

[8] Roffey, B.J., Boggs, S.A., Welsh, H.L.: Infrared studies of quantum diffusion in solid hydrogen. Can. J. Phys. **52**(24), 2451–2453 (1974)

[9] Jen, C.K., Foner, S.N., Cochran, E.L., Bowers, V.A.: Paramagnetic resonance of hydrogen atoms trapped at liquid helium temperature. Phys. Rev. **104**, 846–847 (1956)

[10] Jen, C.K., Foner, S.N., Cochran, E.L., Bowers, V.A.: Electron spin resonance of atomic and molecular free radicals trapped at liquid helium temperature. Phys. Rev. **112**, 1169–1182 (1958)

[11] Bass, A.M., Broida, H.P.: Formation and Trapping of Free Radicals. Academic Press, New York, London (1960)

[12] Andreev, A.F., Lifshitz, I.M.: Quantum theory of defects in crystals. Sov. Phys. JETP **29**, 1107 (1969)

[13] Chester, G.V.: Speculations on bose-einstein condensation and quantum crystals. Phys. Rev. A **2**, 256–258 (1970)

[14] Leggett, A.J.: Can a solid be "superfluid"? Phys. Rev. Lett. **25**, 1543–1546 (1970)

[15] Kagan, Y., Maksimov, L.A., Prokof'ev, N.V.: Quantum diffusion and recombination of atoms in a crystal at low-temperatures. JETP Lett. **36**(6), 253–256 (1982)

[16] Kagan, Y., Maksimov, L.A.: Quantum diffusion in irregular crystals. Sov. Phys JETP **57**, 459 (1983)

[17] Katunin, A.Y., Lukashevich, I.I., Orozmamatov, S.T., Sklyarevskii, V.V., Suraev, V.V., Filippov, V.V., Filippov, N.I., Shevtsov, V.A.: Temperature dependence of the recombination rate constant of hydrogen atoms in solid H_2 at 1.5 K < T < 5.5 K. JETP Lett. **34**, 357 (1981)

[18] Ivliev, A.V., Katunin, A.Y., Lukashevich, I.I., Sklyarevskii, V.V., Suraev, V.V., Filippov, V.V., Filippov, N.I., Shevtsov, V.A.: Temperature dependence of quantum diffusion of h atoms in solid H_2 in the temperature range 1.35K $\leq$T$\leq$4.2 K. JETP Lett. **36**(11), 472 (1982)

[19] Ivliev, A.V., Katunin, A.Y., Lukashevich, I.I., Sklyarevskii, V.V., Suraev, V.V., Filippov, V.V., Filippov, N.I., Shevtsov, V.A.: Investigation of spin-polarized atomic hydrogen in solid H_2 at helium temperatures. JETP **62**(6), 1268 (1985)

[20] Ahokas, J., Järvinen, J., Khmelenko, V.V., Lee, D.M., Vasiliev, S.: Exotic behavior of hydrogen atoms in solid H_2 at temperatures below 1 K. Phys. Rev. Lett. **97**(9), 095301–4 (2006)

[21] Khmelenko, V.V., Bernard, E.P., Vasiliev, S.A., Lee, D.M.: Tunnelling chemical reactions of hydrogen isotopes in quantum solids. Russ. Chem. Rev. **76**(12), 1107 (2007)

[22] Ahokas, J., Vainio, O., Järvinen, J., Khmelenko, V.V., Lee, D.M., Vasiliev, S.: Stabilization of high-density atomic hydrogen in H_2 films at T<0.5 K. Phys. Rev. B **79**(22), 220505 (2009)

[23] Ahokas, J., Vainio, O., Novotny, S., Järvinen, J., Khmelenko, V.V., Lee, D.M., Vasiliev, S.: Magnetic resonance study of H atoms in thin films of H_2 at temperatures below 1 K. Phys. Rev. B **81**, 104516 (2010)

[24] Tsuruta, H., Miyazaki, T., Fueki, K., Azuma, N.: Remarkable isotope effect on production and decay of deuterium and hydrogen atoms in γ-radiolysis of deuterium-hydrogen mixtures at 4 K. A quantum-mechanical tunneling effect. J. Phys. Chem. **87**(26), 5422–5425 (1983)

[25] Miyazaki, T., Lee, K.P., Fueki, K., Takeuchi, A.: Temperature effect on the decay of hydrogen (deuterium) atoms in the radiolysis of solid molecular hydrogen, molecular deuterium, and hydrogen-deuterium molecule (HD) at 4.2 and 1.9 K. evidence for tunneling migration. J. Phys. Chem. **88**(21), 4959–4963 (1984)

[26] Gordon, E.B., Pel'menev, A.A., Pugachev, O.F., Khmelenko, V.V.: Hydrogen and deuterium atoms, stabilized by condensation of an atomic beam in superfluid helium. JETP Lett. **37**(5), 282–285 (1983)

[27] Porter, R.N., Karplus, M.: Potential Energy Surface for H_3. J. Chem. Phys. **40**(4), 1105–1115 (1964)

[28] Takayanagi, T., Masaki, N., Nakamura, K., Okamoto, M., Sato, S., Schatz, G.C.: The rate constants for the $H+H_2$ reaction and its isotopic analogs at low temperatures: Wigner threshold law behavior. J. Chem. Phys. **86**(11), 6133–6139 (1987)

[29] Hancock, G.C., Mead, C.A., Truhlar, D.G., Varandas, A.J.C.: Reaction rates of $H(H)_2$), $D(H_2)$, and $H(D_2)$ van der Waals molecules and the threshold behavior of the bimolecular gas-phase rate coefficient. J. Chem. Phys. **91**(6), 3492–3503 (1989)

[30] Takayanagi, T., Sato, S.: The bending-corrected-rotating-linear-model calculations of the rate constants for the $H+H_2$ reaction and its isotopic variants at low temperatures: The effect of van der Waals well. J. Chem. Phys. **92**(5), 2862 (1990)

[31] Kumada, T.: Experimental determination of the mechanism of the tunneling diffusion of H atoms in solid hydrogen: Physical exchange versus chemical reaction. Phys. Rev. B **68**, 052301 (2003)

[32] Miyazaki, T.: Atom tunneling reactions in quantum solid hydrogen. In: Miyazaki, T. (ed.) Atom Tunneling Phenomena in Physics, Chemistry and Biology. Springer Series on Atomic, Optical, and Plasma Physics, vol. 36, pp. 59–90. Springer, Berlin, Heidelberg (2004)

[33] Katunin, A.Y., Lukashevich, I.I., Orosmamatov, S.T., Sklyarevskii, V.V., Suraev, V.V., Filippov, V.V., Filippov, N.I., Shevtsov, V.A.: The overhauser effect for atomic hydrogen in a solid H_2-matrix. Phys. Lett. A **87**(9), 483–485 (1982)

[34] Miyazaki, T., Mori, S., Nagasaka, T., Kumagai, J., Aratono, Y., Kumada, T.: Decay dynamics of h atoms in solid hydrogen at 4.2 K. controlling factor of tunneling reaction H + para-H2 → para-H2 + H. J. Phys. Chem. A **104**(42), 9403–9407 (2000)

[35] Kumada, T., Mori, S., Nagasaka, T., Kumagai, J., Miyazaki, T.: Resonance effect on the tunneling reaction: $H+H_2=H_2+H$ in solid hydrogen. J. Low. Temp. Phys.

122(3), 265–277 (2001)

[36] Kiselev, S.I., Khmelenko, V.V., Lee, D.M.: Hydrogen atoms in impurity-helium solids. Phys. Rev. Lett. **89**, 175301 (2002)

[37] Widom, A., Richards, M.G.: Quantum theory of diffusion with application to solid helium. Phys. Rev. A **6**, 1196–1199 (1972)

[38] Grigoriev, V.N., Esel'son, B.N., Mikheev, Y.E. V. A. Shulman Sov. Phys. JETP Lett. **17**, 16 (1973)

[39] Constable, J.H., Gaines, J.R., Sokol, P.E., Souers, P.C.: Production of h atoms in solid H_2 by rf discharge. J. Low Temp. Phys. **58**, 467 (1985)

[40] Shevtsov, V., Frolov, A., Lukashevich, I., Ylinen, E., Malmi, P., Punkkinen, M.: The ortho-to-para conversion in solid hydrogen, catalyzed by hydrogen atoms. J. Low Temp. Phys. **95**(5), 815–833 (1994)

[41] Strom, A.I., Fillmore, K.L., Anderson, D.T.: Hydrogen atom catalyzed ortho-to-para conversion in solid molecular hydrogen. Low Temp. Phys. **45**(6), 676–688 (2019)

[42] Mutunga, F.M., Follett, S.E., Anderson, D.T.: Communication: H-atom reactivity as a function of temperature in solid parahydrogen: The H + N_2O reaction. J. Chem. Phys. **139**(15), 151104 (2013)

[43] Paulson, L.O., Mutunga, F.M., Follett, S.E., Anderson, D.T.: Reactions of atomic hydrogen with formic acid and carbon monoxide in solid parahydrogen i: Anomalous effect of temperature. J. Phys. Chem. A **118**(36), 7640–7652 (2014)

[44] Strom, A.I., Gutiérrez-Quintanilla, A., Chevalier, M., Ceponkus, J., Crépin, C., Anderson, D.T.: Matrix isolation spectroscopy and nuclear spin conversion of propyne suspended in solid parahydrogen. J. Phys. Chem. A **124**(22), 4471–4483 (2020)

[45] Sheludiakov, S., Lee, D.M., Khmelenko, V.V., Järvinen, J., Ahokas, J., Vasiliev, S.: Purely spatial quantum diffusion of H atoms in solid H_2 at temperatures below 1 K. Phys. Rev. Lett. **126**, 195301 (2021)

[46] Sheludiakov, S., Lee, D.M., Khmelenko, V.V., Dmitriev, Y.A., Järvinen, J., Ahokas, J., Vasiliev, S.: Purely spatial diffusion of H atoms in solid normal- and para-hydrogen films. Phys. Rev. B **105**, 144102 (2022)

[47] Sheludiakov, S., Wetzel, C.K., Lee, D.M., Khmelenko, V.V., Järvinen, J., Ahokas, J., Vasiliev, S.: Studies of accumulation rate of H atoms in solid H_2 films exposed to 0.1 and 5.7 keV electrons. Phys. Rev. B **107**, 134110 (2023)

[48] Sheludiakov, S., Ahokas, J., Vainio, O., Järvinen, J., Zvezdov, D., Vasiliev, S.,

Khmelenko, V.V., Mao, S., Lee, D.M.: Experimental cell for molecular beam deposition and magnetic resonance studies of matrix isolated radicals at temperatures below 1 K. Rev. Sci. Instrum. **85**(5), (2014)

[49] Sheludiakov, S., Lee, D.M., Khmelenko, V.V., Järvinen, J., Ahokas, J., Vasiliev, S.: Experimental cell with a Fabry–Pérot resonator tuned in situ for magnetic resonance studies of matrix-isolated radicals at temperatures below 1 K. Rev. Sci. Instrum. **91**(6), 063901 (2020)

[50] Vasilyev, S., Järvinen, J., Tjukanoff, E., Kharitonov, A., Jaakkola, S.: Cryogenic 2 mm wave electron spin resonance spectrometer with application to atomic hydrogen gas below 100 mK. Rev. Sci. Instrum. **75**(1), 94–98 (2004)

[51] Järvinen, J., Khmelenko, V.V., Lee, D.M., Ahokas, J., Vasiliev, S.: Atomic hydrogen in thick H_2 films at temperatures 0.05-2 K. J. Low Temp. Phys. **162**(3), 96–104 (2011)

[52] Collins, G.W., Souers, P.C., Maienschein, J.L., Mapoles, E.R., Gaines, J.R.: Atomic-hydrogen concentrations in solid D-T and T_2. Phys. Rev. B **45**, 549–556 (1992)

[53] Kumada, T., Sakakibara, M., Nagasaka, T., Fukuta, H., Kumagai, J., Miyazaki, T.: Absence of recombination of neighboring H atoms in highly purified solid parahydrogen: Electron spin resonance, electron-nuclear double resonance, and electron spin echo studies. J. Chem. Phys. **116**(3), 1109–1119 (2002)

[54] Van Kranendonk, J., Karl, G.: Theory of the rotational and vibrational excitations in solid parahydrogen, and frequency analysis of the infrared and raman spectra. Rev. Mod. Phys. **40**, 531–555 (1968)

[55] Kuo, C.-Y., Kerl, R.J., Patel, N.D., Patel, C.K.N.: Nonradiative relaxation of excited vibrational states of solid hydrogen. Phys. Rev. Lett. **53**, 2575–2578 (1984)

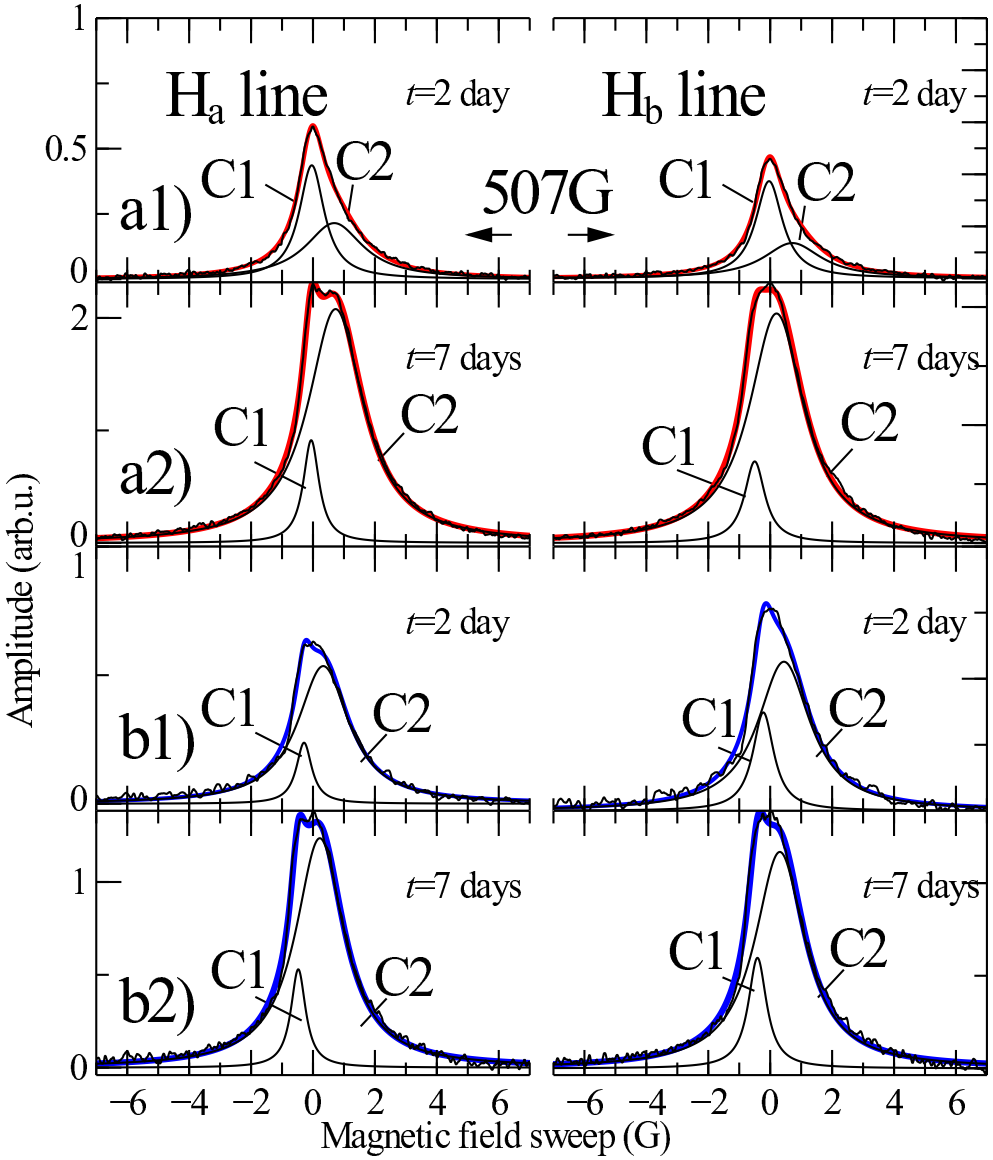

Fig. 4 ESR spectra of H atoms in 2.5 μm normal (a1 and a2) and para (b1 and b2) molecular hydrogen films (black lines). Spectra were taken after 2 days (a1 and b1) and after 7 days (a2 and b2) following film preparation. Experimental lines can be fitted as a sum of two Lorentzian lines, narrow C1 and broad C2. The sum of these fit lines shown with solid red lines for normal hydrogen film and with blue lines for para-hydrogen films.

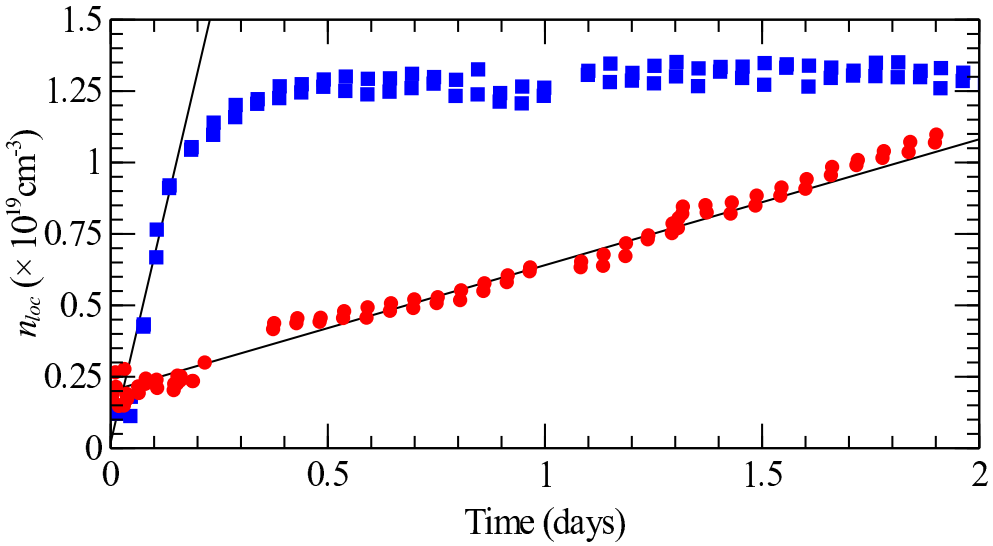

Fig. 5 Dependence of local concentration of hydrogen atoms during early stage of accumulation in normal (red filled circles) and in para-(blue filled squares) H_2 solid films.

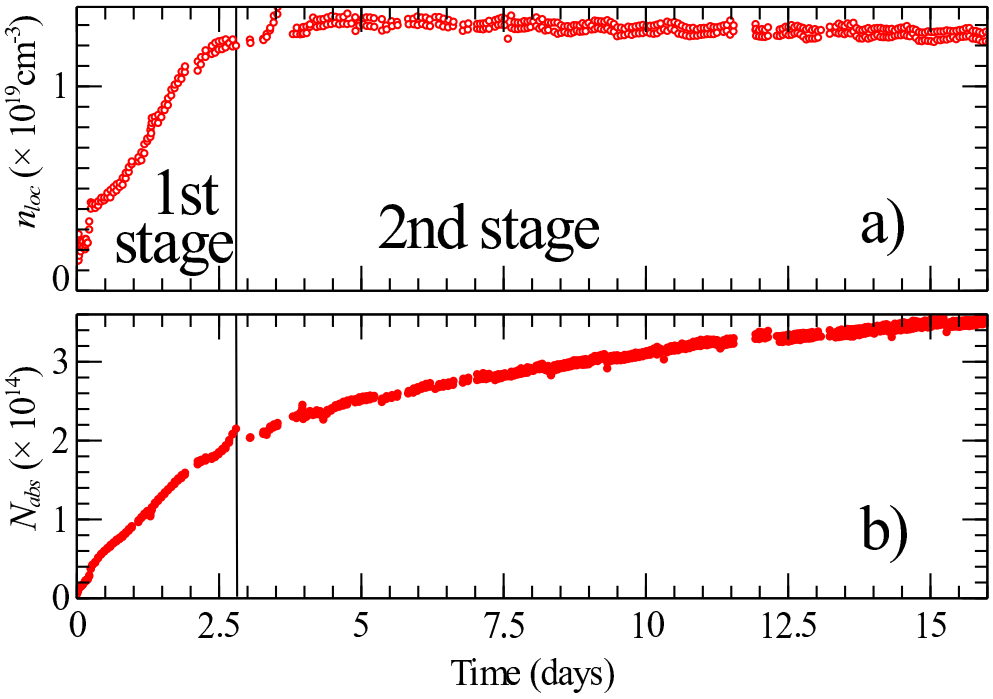

Fig. 6 a) Time dependence of the local concentration of H atoms in normal H_2 film (open red circles). b) Time dependence of the absolute number of H atoms in normal H_2 film (filled red circles).

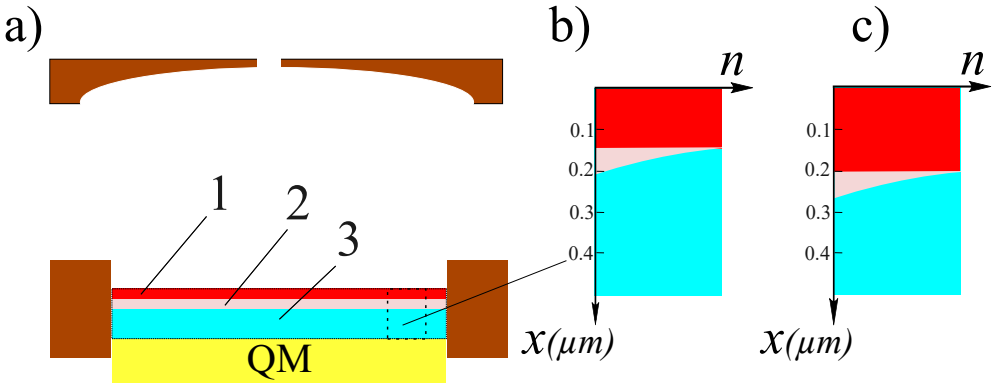

Fig. 7 Schematic of the H_2 film grown on the lower flat ESR mirror. a) 1. A high-concentration layer of H atoms (100 nm) formed during the first stage of accumulation (red) 2. Low-concentration layer of H atoms (pink) in the front of high-concentration layer. 3. H_2 solid film (blue color) empty of H atoms. b) An H-atom concentration profile after 2 days of accumulation and corresponding to Fig. 4a1. c) An H-atom concentration profile after 7 days of accumulation and corresponding to Fig. 4a2.

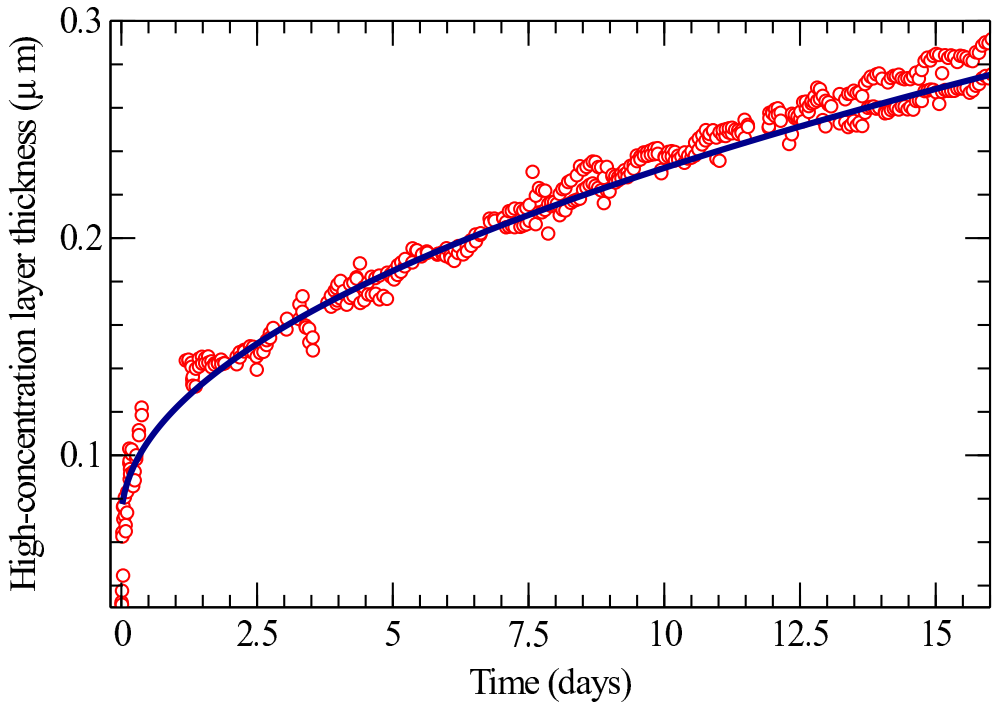

Fig. 8 A dependence of the H atom high-concentration layer thickness on time in the normal H_2 film showing the H-atom spatial diffusion (red open circles). Solid line represents a fit according to the experimental data using Eq. (6).

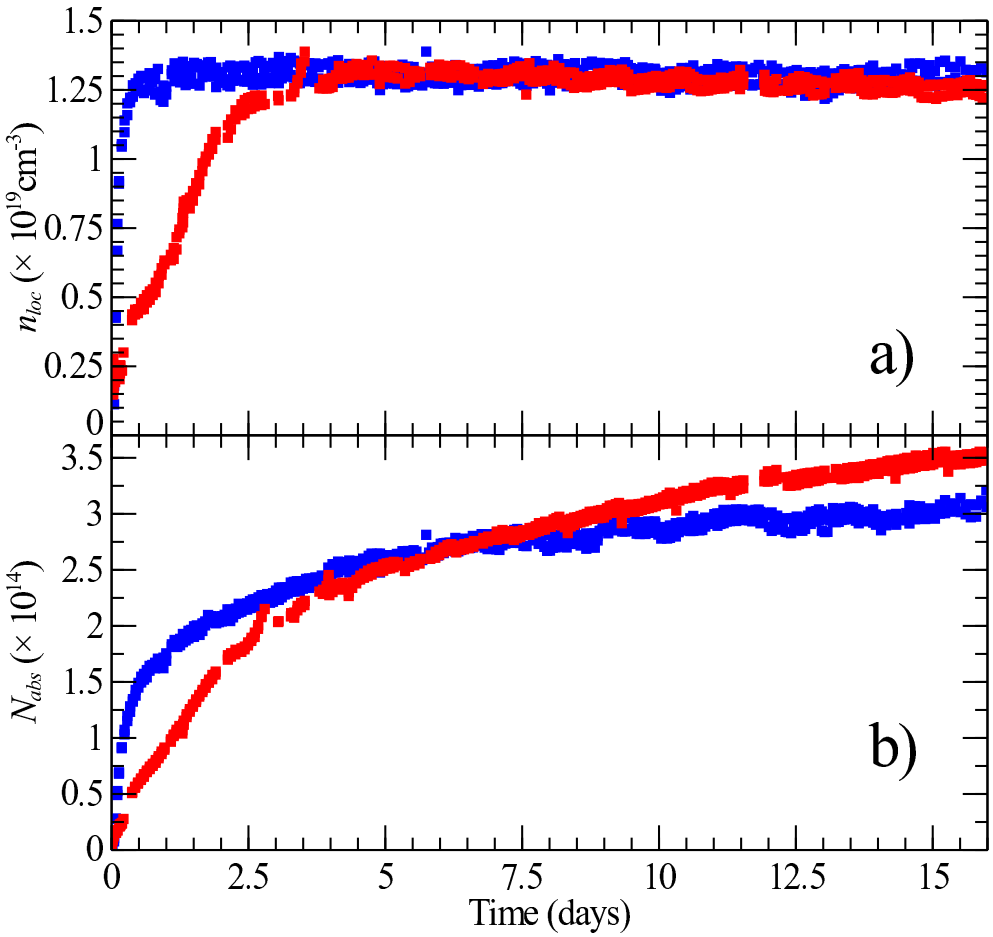

Fig. 9 Time evolution of the local concentrations of H atoms (a) and the absolute number of H atoms (b) in the normal H_2 (red filled squares) and para-H_2 (blue filled squares) 2.5 μm films.

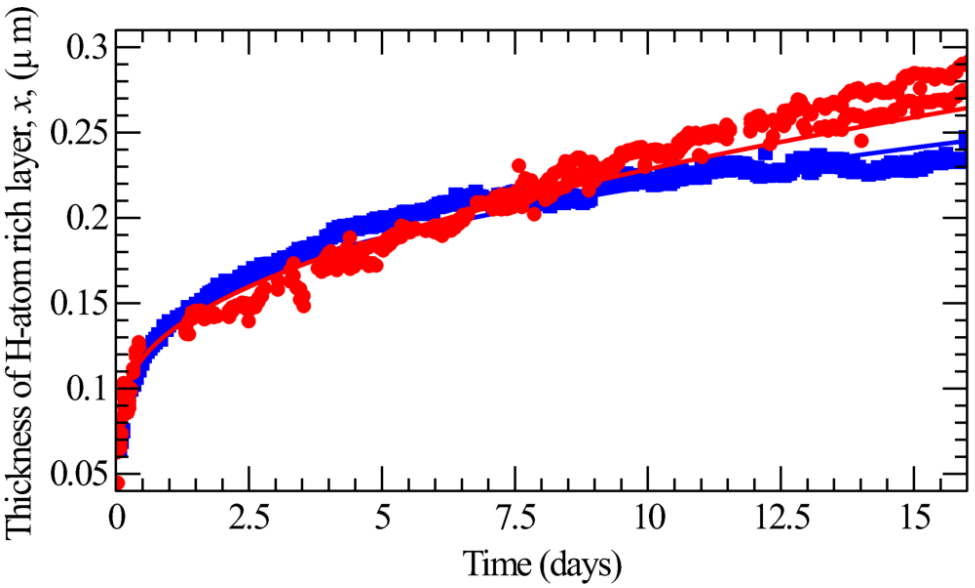

Fig. 10 Time evolution of the thickness of the high-concentration layer of H atoms in normal H_2 (red closed circles) and para H_2 (blue filled squares) films. Blue and red solid lines represent the fits according to the experimental data using Eq. (6).